A visco-hyperelastic constitutive model and its application in bovine tongue tissue

Ali-Akbar Karkhaneh Yousefi, Mohammad Ali Nazari, Pascal Perrier, Masoud Shariat Panahi, Yohan Payan

▶ **To cite this version:**

Ali-Akbar Karkhaneh Yousefi, Mohammad Ali Nazari, Pascal Perrier, Masoud Shariat Panahi, Yohan Payan. A visco-hyperelastic constitutive model and its application in bovine tongue tissue. Journal of Biomechanics, 2018, 71, pp.190-198. 10.1016/j.jbiomech.2018.02.008 . hal-01744059

HAL Id: hal-01744059
https://hal.science/hal-01744059

Submitted on 27 Mar 2018

HAL is a multi-disciplinary open access archive for the deposit and dissemination of scientific research documents, whether they are published or not. The documents may come from teaching and research institutions in France or abroad, or from public or private research centers.

L'archive ouverte pluridisciplinaire **HAL**, est destinée au dépôt et à la diffusion de documents scientifiques de niveau recherche, publiés ou non, émanant des établissements d'enseignement et de recherche français ou étrangers, des laboratoires publics ou privés.

A Visco-hyperelastic Constitutive Model and its Application in Bovine Tongue Tissue

Ali-Akbar Karkhaneh Yousefi [a], Mohammad Ali Nazari [a], Pascal Perrier [b],
Masoud Shariat Panahi [a], Yohan Payan [c]

[a] *School of Mechanical Engineering, College of Engineering, University of Tehran, Tehran, Iran*
[b] *Univ. Grenoble Alpes, CNRS, Grenoble INP, Gipsa-lab, F38000 Grenoble France*
[c] *Univ. Grenoble Alpes, CNRS, Grenoble INP, TIMC-IMAG, F38000 Grenoble France*

Abstract

Material properties of the human tongue tissue have a significant role in understanding its function in speech, respiration, suckling, and swallowing. Tongue as a combination of various muscles is surrounded by the mucous membrane and is a complicated architecture to study. As a first step before the quantitative mechanical characterization of human tongue tissues, the passive biomechanical properties in the superior longitudinal muscle (SLM) and the mucous tissues of a bovine tongue have been measured. Since the rate of loading has a sizeable contribution to the resultant stress of soft tissues, the rate dependent behavior of tongue tissues has been investigated via uniaxial tension tests (UTTs). A method to determine the mechanical properties of transversely isotropic tissues using UTTs and inverse finite element (FE) method has been proposed.

Assuming the strain energy as a general nonlinear relationship with respect to the stretch and the rate of stretch, two visco-hyperelastic constitutive laws (CLs) have been proposed for isotropic and transversely isotropic soft tissues to model their stress-stretch behavior. Both of them have been implemented in ABAQUS explicit through coding a user-defined material subroutine called VUMAT and the experimental stress-stretch points have been well tracked by the results of FE analyses. It has been demonstrated that the proposed laws make a good description of the viscous nature of tongue tissues. Reliability of the proposed models has been compared with similar nonlinear visco-hyperelastic CLs.

Keywords: Bovine tongue tissue, Visco-hyperelasticity, Passive behavior, Transversely isotropic, inverse finite element method.

1. Introduction

Soft tissues envelope, bind, and connect other parts of the body (Kulkarni et al. 2016). From a mechanical point of view, soft tissues exhibit nonlinear stress-strain behavior, strain rate sensitivity, hysteresis, viscoelastic responses (relaxation and creep), and permanent strains. They have been extensively studied using continuum mechanics and nonlinear elasticity (Humphrey 2003 and Holzapfel et al. 2010).

The tongue is one of the most intriguing human soft tissues because it plays a vital role in respiration, suckling, acquiring and manipulating food, swallowing, and speech. Obviously, not all species use the tongue in the same way, so this organ has evolved to generate deformations into various shapes and mechanisms of movement (McLoon et al. 2012). Especially, human tongue experiences finite strains with high rates during speech production (Gerard et al. 2005 and Rastadmehr et al. 2008).

The mammalian tongue is a complex muscular organ which is composed of the mucous membrane, intrinsic and extrinsic muscles (McLoon et al. 2012). Extrinsic muscles originate on structures external to

the tongue like bones and insert into the body of the tongue: the genioglossus, the hyoglossus, the styloglossus, the geniohyoid and the palatoglossus. These muscles help the tongue to move in any directions. Intrinsic muscles are fully embedded in the body of the tongue and determine the shape of the tongue: the superior longitudinal, the inferior longitudinal, the verticalis and the transversalis (Gerard et al. 2003).

The muscular tissues have been frequently considered as a network of muscle fibers embedded in an isotropic matrix (Hernández et al. 2011). Skeletal muscles are composed of 70-80% of water so they are usually considered to be incompressible (Takaza et al. 2013). The main course of the fibers determines one of the directions of material anisotropy and such fibers may be considered as transversely isotropic or orthotropic materials (Martin et al. 1998 and 2006). Mechanical behavior of the skeletal muscles can be characterized by their passive and active responses. The passive response can be modeled within the framework of hyperelasticity. The active response which is due to the contractile behavior of the muscle fibers can be represented by some muscle models like Hill-type characteristic behavior's (Nazari 2011, Martin et al. 1998).

The tongue has been widely investigated experimentally and numerically to describe its actions in the human body (Gerard et al. 2003, Tricarico 1995, Dang and Honda 2002, Vogt 2005 and Fujita et al. 2007). The developed FE models intend to improve the understanding of the role of the tongue in linguistics. Kajee et al. (2013) developed a linear elastic FE model of the tongue tissue to better understand its actions in the obstructive sleep apnea syndrome. Using an indentation test, Gerard et al. (2003) proposed an isotropic hyperelastic model of the tongue to investigate its role in speech production. Unfortunately, complex behavior of the tongue tissue has been reduced by much simpler models in previous researches. Due to the lack of experiments, a CL considering the nonlinear nature of tongue tissues, their time dependent response and anisotropic behavior has not been proposed yet.

In higher order mammals, the musculatures of tongues are similar (Gilbert et al. 2006 and McLoon et al. 2012). It was therefore decided to focus this paper on bovine tongue tissues since it is still complicated to characterize the biomechanical properties of human tongue tissues. Regarding the distinct ability of the bovine tongue which wraps around the grass and heaves to rip it off, it was hypothesized that both of the human and the bovine tongue tissue have similar passive constitutive behavior. This unique function of the bovine tongue is probably due to the fact that the capacity of producing the active force in the muscles of the bovine tongue is more than the human one.

To characterize the mechanical properties of the bovine tongue tissue, the rate dependent and fiber oriented responses of bovine tongue tissue are measured under UTTs. Furthermore, two accurate and reliable visco-hyperelastic CLs are proposed for the passive behavior of isotropic and transversely isotropic soft tissues. Also, in comparison to the well-known CLs, the accuracy of the proposed model in approximating the experimental data is demonstrated.

2. Tests Procedure

In order to accurately measure the mechanical properties of the bovine tongue tissue, four freshly slaughtered adult bovine tongues were provided. The sacrifice has been done early morning. Immediately after the sacrifice, the tongue was cut from the larynx and immersed in a saline solution at $4^{\circ}C$ to keep it fresh and prevent its degradation (Hernández et al. 2011 and Gras et al. 2012). Due to the complex structure and the direction variation of tongue fibers (Gilbert et al. 2006), cutting an appropriate sample with a fixed fiber direction from each muscle part is difficult in practice. So in the current research, the samples were cut from the mucous membrane and the SLM tissue. The length to width ratio of the samples was at least around 8. These samples underwent a UTT on a Santam STM-1 machine with a 6 kg full-scale load cell. All of the reported data in this paper have been averaged among the measured stress-stretch behavior in

different samples dissected from four bovine tongues. Figure 1 shows the bovine tongue and a corresponding sample during a tensile test.
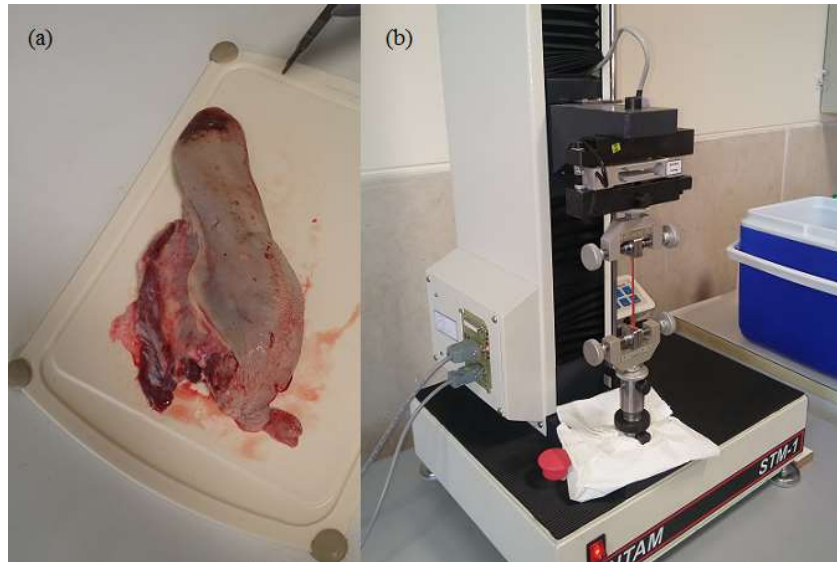

Figure 1. Bovine tongue (a) and a sample of the superior longitudinal muscle under uniaxial tension test (b).

2.1 Mucous Membrane

The mucous membrane has mainly an isotropic structure, so its mechanical properties should be easier to obtain than for tongue muscles. With the aid of a surgical blade, the mucous was separated from the muscles at the tip of the tongue, then some samples were dissected from it. Tests were performed at four different strain rates to measure the elastic and viscoelastic components. Each reported stress-stretch curve for the mucous tissue represents the average measured stress in five samples.

2.2 SLM

The SLM is a thin layer of muscle fibers along the tongue axis that located below the mucous membrane and covers the tongue body. In the bovine tongue tissue, the SLM is combined with the fat tissues in the posterior regions and has a variable thickness in the frontal planes in the anterior regions. So, it is very difficult to dissect a sample from the SLM with 90° and even 45° to the fibers alignment that can be used experimentally. Therefore, in this research, the measurement of the mechanical response of the SLM was limited to the samples aligned with 0°, 20°, and 35° with respect to the fibers' direction.

At the upper surface of the bovine tongue, fibers have a fixed direction along the SLM; our samples were therefore cut from this region. Response of the SLM tissue to the UTTs strongly depends on the angle between the direction of the fibers and the tensile force. To measure this dependency, samples were chosen parallel to the fibers direction and 20° with respect to them. Six samples along the fibers direction, four samples at 20° to the fibers, and two samples at 35° to the fibers were prepared to measure the average response in the SLM tissue. As for the mucous tissues, tests were performed at different strain rates to quantify the viscous contribution of stress.

3. Constitutive Model

A CL has to be chosen to describe the stress-strain relationship of the tissues. Chagnon et al. (2015) reviewed and classified the most popular hyperelastic CLs. Among the many CLs proposed in the literature,

those which consider the strain rate as an explicit variable have provided better predictions of viscous behavior especially at higher strain rates (Pioletti et al. 1998, 2000 and 2006). Furthermore, the domain of validity of other visco-hyperelastic constitutive models, like Fung's quasi-linear viscoelastic law (Fung 2013) and Holzapfel's model (Holzapfel 2000), have been restricted to low strain rates (Pioletti et al. 1998, Limbert et al. 2004, Zhurov et al. 2007 and Lu et al. 2010).

In this research, the nonlinearity of the stress-strain curves and their dependence on the strain rate are incorporated in the strain energy function through the introduction of powers of strain rates as independent explicit variables.

3.1. Kinematics

Let $\mathbf{X}$ and $\mathbf{x}$ be the position vector of material points in the reference (undeformed) and deformed configuration, respectively. The deformation gradient tensor, $\mathbf{F}$, of any function χ, describing the motion $\mathbf{x} = \chi(\mathbf{X}, t)$, is given by

$$\mathbf{F} = \frac{\partial \mathbf{x}}{\partial \mathbf{X}} \tag{1}$$

which maps any position vector of the reference configuration to the deformed configuration. The right Cauchy-Green strain tensor is given by $\mathbf{C} = \mathbf{F}^{\mathrm{T}}\mathbf{F}$. For three dimensional hyperelastic CLs representing isotropic materials, it is common to use the invariants of a material strain tensor as variables instead of the components of the tensor itself. So, taking $\mathbf{C}$ as this material tensor, its three principal invariants are defined as

$$I_1 = tr(\mathbf{C}), \quad I_2 = \frac{1}{2}[tr(\mathbf{C})^2 - tr(\mathbf{C}^2)], \quad I_3 = det(\mathbf{C}) = J^2 \tag{2}$$

in which J is the Jacobian and represents the ratio of volume change during the deformation. For materials reinforced with one family of fibers, the principal invariants defined by equation (2) are not sufficient to describe the behavior. Hence, for transversely isotropic materials with a preferred fiber direction specified by the unit vector $\mathbf{N}$ in the reference configuration, the structural tensor $\mathbf{A}$ and two additional invariants $I_{4,5}$ are defined as:

$$\mathbf{A} = \mathbf{N} \otimes \mathbf{N} \tag{3a}$$
$$I_4 = tr(\mathbf{C}\mathbf{A}), \quad I_5 = tr(\mathbf{C}^2\mathbf{A}) \tag{3b}$$

where $\otimes$ represents the dyadic multiplication of two vectors (Spencer 1984).

It can be easily shown that the rate of the deformation gradient tensor, $\dot{\mathbf{F}}$, and the velocity gradient tensor, $\mathbf{l}$, are related as:

$$\dot{\mathbf{F}} = \mathbf{l}\mathbf{F} \tag{4}$$

So, the rate of $\mathbf{C}$ can be shown to be $\dot{\mathbf{C}} = 2\mathbf{F}^{\mathrm{T}}\mathbf{d}\mathbf{F}$ where the tensor $\mathbf{d}$ is the symmetric part of $\mathbf{l}$. As for $\mathbf{C}$, the use of the invariants of $\dot{\mathbf{C}}$ are often preferred to propose CLs for viscoelastic materials. In general, for a transversely isotropic material, 12 invariants $(J_1, J_2, \ldots, J_{12})$ of $\dot{\mathbf{C}}$ have been defined (Boehler 1987). Among them, J_2 and J_5 are the most popular invariants in the proposed viscoelastic CLs for isotropic and transversely isotropic materials, respectively (Pioletti et al. 1998, Limbert et al. 2004, Zhurov et al. 2007, Lu et al. 2010, Kulkarni et al. 2016 and Ahsanizadeh and LePing 2015):

$$J_2 = \frac{1}{2}tr(\dot{\mathbf{C}}^2), \qquad J_5 = \mathbf{N}.\dot{\mathbf{C}}^2\mathbf{N} \tag{5}$$

Their derivatives with respect to the $\dot{\mathbf{C}}$ have been presented by Limbert et al. (2004).

3.2. Stress

In hyperelasticity, it is postulated that a scalar valued free energy function exists which is called the Helmholtz free energy function. In thermally independent processes, the rate of Helmholtz free energy

function is equivalent to the rate of elastic potential $\psi^e(\mathbf{C}, \mathbf{A})$. In order to include the loading rate effects in the resultant stress, $\dot{\mathbf{C}}$ can be considered as an explicit variable in the stress definition, like $\mathbf{S} = \mathbf{S}(\mathbf{C}, \dot{\mathbf{C}})$, where $\mathbf{S}$ is the second Piola-Kirchhoff stress tensor.

For isothermal process, the thermodynamical principles reduce to the satisfaction of the Clausius-Duhem inequality

$$\left(\mathbf{S} - 2\frac{\partial \psi^e}{\partial \mathbf{C}}\right) : \frac{\dot{\mathbf{C}}}{2} \geq 0 \quad \forall \mathbf{C}, \dot{\mathbf{C}} \tag{6}$$

in which : represents the double contraction of two tensors. Without energy dissipation, Pioletti et al. (1998) showed that $\mathbf{S} = \mathbf{S}^e = 2\frac{\partial \psi^e}{\partial \mathbf{C}}$ can be a solution for equation (6), where $\mathbf{S}^e$ is the elastic part of stress.

In the existence of dissipation, potential viscous function $\psi^v(\mathbf{C}, \dot{\mathbf{C}}, \mathbf{A})$ was defined as $2\frac{\partial \psi^v}{\partial \dot{\mathbf{C}}} = \mathbf{S} - 2\frac{\partial \psi^e}{\partial \mathbf{C}}$. So, the Clausius-Duhem inequality can be written as

$$\frac{\partial \psi^v}{\partial \dot{\mathbf{C}}} : \dot{\mathbf{C}} \geq 0 \quad \forall \dot{\mathbf{C}} \tag{7}$$

which is valid for all continuous, non-negative and convex ψ^v (Pioletti et al. 1998). So, for a viscoelastic material, the stress tensor can be represented by

$$\mathbf{S} = 2\frac{\partial \psi^e}{\partial \mathbf{C}} + 2\frac{\partial \psi^v}{\partial \dot{\mathbf{C}}} = \mathbf{S}^e + \mathbf{S}^v \tag{8}$$

where the first term is the quasi-static part of the response and the second term represents the rate dependent measure of the material response in loading.

3.3. CLs

In the current research, two CLs for better prediction of the viscoelastic behavior of soft tissues are presented. Inspired by Vogel et al. (Vogel et al. 2017), these CLs are in the viscous potential part and model the isotropic and transversely isotropic behaviors. In the isotropic case, constitutive models are proposed as:

$$\psi^e = p(J-1) + \frac{c_1}{c_2}\left(e^{c_2(I_1-3)} - 1\right) \tag{9a}$$

$$\psi^v = c_3 J_2 (I_1 - 3)^{c_4} \tag{9b}$$

with the Lagrangean multiplier p and the material parameters (MPs) c_{1-4}, in which all of them must have non-negative values to warrant the convexity condition of ψ^e and ψ^v. In ψ^e, the first term ensures the incompressibility constraint of soft tissues.

In the case of a transversely isotropic material, a particular elastic potential function $\psi^e = \psi^e(I_1, J, I_4)$ and a viscous potential function $\psi^v = \psi^v(J_5)$ are proposed as (for $I_4 > 1$):

$$\psi^e = p(J-1) + c_1(I_1 - 3)^2 + \frac{c_2}{c_3}(I_4 - 1)^{c_3} \tag{10a}$$

$$\psi^v = c_4 J_5 (I_4 - 1)^{c_5} \tag{10b}$$

with the MPs c_{1-5}, in which all of them have to be non-negative to warrant the convexity condition. For ψ^e, the second term is added to take into account the contribution of the matrix-fiber ensemble in a transversely isotropic material, and the third term accounts for the fibers' resistance to elongation. In order to reduce the number of MPs, the viscoelastic behavior only considers fibers resistance to loadings. Similar to term $J_2(I_1 - 3)^{c_4}$ in equation (9b), the term $J_5(I_4 - 1)^{c_5}$ provides a zero value for ψ^v in the reference configuration and ensures a nonlinear relationship for the stress as a function of the strain and strain rate.

The idea of proposing such potential viscous functions is based on the previous viscoelastic models for long-time behavior (creep and stress relaxation) of soft tissues (Davis and Vita 2012 and 2014, Pena et al. 2011). In order to improve the accuracy of the quasi-linear viscoelastic (QLV) models, it has been

demonstrated that the characteristic time constants and dimensionless coefficients of the Prony series have to be considered as a nonlinear function of strain. So, similar to the long-time responses, the rate dependent (short-time) responses of soft tissues must be strongly dependent on the strain. The use of power c_5 in equation (10b) and power c_4 in (9b) ensures the existence of a general nonlinear dependency of stress to strain in the proposed CLs.

For the proposed model in equation (9), the elastic and viscoelastic part of $\mathbf{S}$ are given by:

$$\mathbf{S}^e = p\mathbf{C}^{-1} + 2c_1 e^{c_2(I_1-3)}\mathbf{I} \tag{11a}$$

$$\mathbf{S}^v = 2c_3(I_1 - 3)^{c_4}\dot{\mathbf{C}} \tag{11b}$$

in which $\mathbf{I}$ represents the second order identity tensor. With the use of equation (10), the similar relationships for stress can be obtained as:

$$\mathbf{S}^e = p\mathbf{C}^{-1} + 4c_1(I_1 - 3)\mathbf{I} + 2c_2(I_4 - 1)^{(c_3-1)}\mathbf{A} \tag{12a}$$

$$\mathbf{S}^v = 2c_4(I_4 - 1)^{c_5}(\mathbf{N}\otimes\dot{\mathbf{C}}\mathbf{N} + \mathbf{N}\dot{\mathbf{C}}\otimes\mathbf{N}). \tag{12b}$$

Figure 2 represents a fully incompressible sample with fibers along the direction of unit vector $\mathbf{N}$ with zero component out of the E1E2 plane. When this sample is loaded along the E1 direction, $\mathbf{F}$ can be written as (Ogden 2009):

$$\mathbf{F} = \begin{bmatrix} F_{11} & F_{12} & 0 \\ F_{21} & F_{22} & 0 \\ 0 & 0 & F_{33} \end{bmatrix} \tag{13}$$
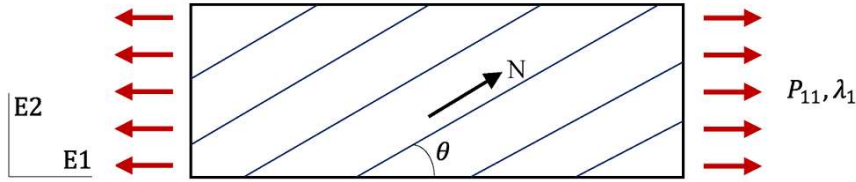

Figure 2. A transversely isotropic sample under uniaxial tension. Fibers are supposed to be fully laid in the E1E2 plane.

in which the off-diagonal components vanish only for $\theta = 0°$ and $\theta = 90°$; $F_{33} = 1/F_{11}F_{22}$ due to incompressibility assumption. Thus, using the relationship $\mathbf{P} = \mathbf{FS}$, from equation (12) and (13) the components of the nominal stress tensor $\mathbf{P}$ can be obtained as a function of the components of $\mathbf{F}$ and $\dot{\mathbf{F}}$. Also, the traction free boundary conditions in E3 direction leads to an equation, from which the unknown pressure p can be computed. In general, it is not possible to determine all the components of $\mathbf{F}$ for an arbitrary θ. For $\theta \neq 0°$ sample undergoes shear stress in the E1E2 plane. Therefore, there is no explicit relationship between the stress and the controllable parameters of the machine. Thus, a inverse FE method has to be used next to the experimental data points to determine the uncontrollable components of $\mathbf{F}$.

To calculate the time derivative of $\mathbf{F}$ to be used in the FE analysis (FEA), let the deformation gradient tensors at the beginning and at the end of a time increment $\Delta t = t - t_0$ be $\mathbf{F}_{t_0}$ and $\mathbf{F}_t$, respectively. A fully implicit time integration of equation (4) yields (Li et al. 2004):

$$\mathbf{F}_t = exp(\Delta t \mathbf{l}_t)\mathbf{F}_{t_0} \tag{14}$$

in which $\mathbf{l}_t$ represents the velocity gradient tensor at time t. For sufficiently small Δt, equation (14) can be approximated by:

$$\mathbf{F}_t \cong (\mathbf{I} + \Delta t \mathbf{l}_t)\mathbf{F}_{t_0} \tag{15}$$

Thus, by use of the calculated velocity gradient tensor from equation (15) in equation (4), $\dot{\mathbf{F}}$ can be computed.

Also, from equation (11) the horizontal component of $\mathbf{P}$, which undergoes a symmetric deformation in E2 and E3 directions, $\lambda_2 = \lambda_1^{-0.5}$, can be obtained as:

$$P_{11}^e = p\lambda_1^{-1} + 2c_1\lambda_1 e^{c_2(\lambda_1^2 + 2\lambda_1^{-1} - 3)} \tag{16a}$$

$$P_{11}^v = 4c_3\lambda_1^2\dot{\lambda}_1(\lambda_1^2 + 2\lambda_1^{-1} - 3)^{c_4} \tag{16b}$$

To show the accuracy of the proposed models in predicting the rate dependent behavior, they are compared with one of the most popular transversely isotropic visco-hyperelastic CLs for soft tissues (Limbert et al. 2004 and 2007, Lu et al. 2010 and Kulkarni et al. 2016), originally proposed by Limbert et al. (2004):

$$\psi^v = a_1 J_2(I_1 - 3) + a_2 J_5(I_4 - 1)^2 \tag{17}$$

a_{1-2} being non-negative MPs. The second term in equation (17) is not considered for isotropic materials.

4. Numerical Results

In this section, the two CLs proposed to model viscoelastic soft tissues are compared to experimental data collected on different parts of bovine tongue tissue. At first, the elastic MPs have to be determined independently of the viscoelastic MPs by ignoring the potential viscous functions. Then, the viscoelastic MPs can be estimated from one of the tests at a non-zero strain rate. For the mucous tissue, the quasi-static response of the proposed model can be approximated by equation (16a). So, parameters $c_{1,2}$ can be obtained by fitting equation (16a) to the elastic stress-stretch response via a MATLAB script according to the Levenberg–Marquardt optimization algorithm. Similarly, the viscous material parameters $c_{3,4}$ and a_1 are estimated by fitting both models to the experimental data points at a strain rate of 1.46%/s. Table 1 compares the results of the parameters estimation for the mucous tissue when our proposed CL is assumed from one side, and with the use of the Limbert's model from the other side. Figure 3 plots nominal stress versus stretch for the elastic loading and strain rate of 1.46%/s in the mucous tissue. In this figure, the coefficient of determination R^2 as a measurement of goodness of fitting shows that in the both models the MPs are well-defined to follow the experimental points.

Table 1. Mucous tissue material parameters estimations for the proposed model and for Limbert's model.

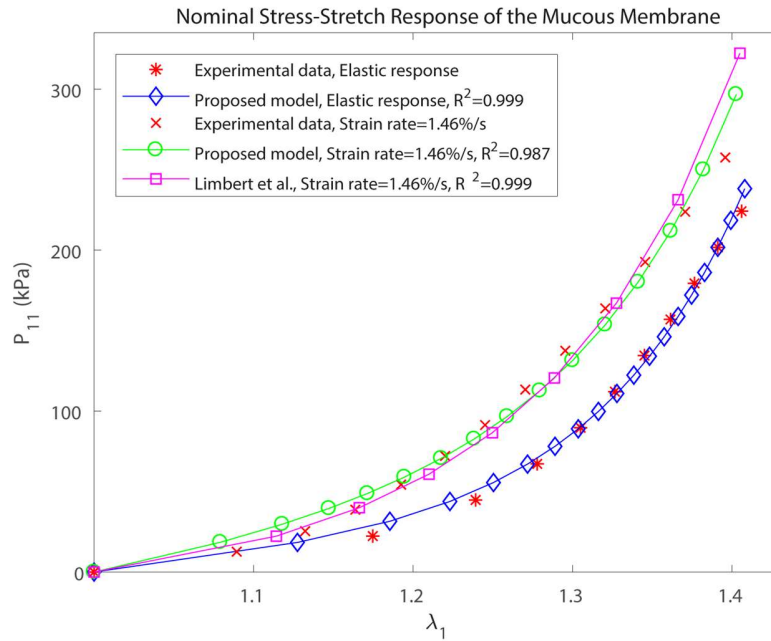|	c_1 (kPa)	c_2 (-)	c_3 (kPa)	c_4 (-)	a_1 (kPa)
Proposed model	22.09	4.433	1016	0.606	-
Limbert et al.	22.09	4.433	-	-	1870

Figure 3. Behavior of the mucous tissue under uniaxial tensile tests and the fitted constitutive laws.

Using the estimated MPs, the behavior of the mucous tissue was predicted at different strain rates of 5.46%/s and 6.60%/s. As can be seen from the coefficient of determinations in figure 4, our model provides a slightly better prediction than Limbert's model on the viscoelastic behavior of the mucous tissue.
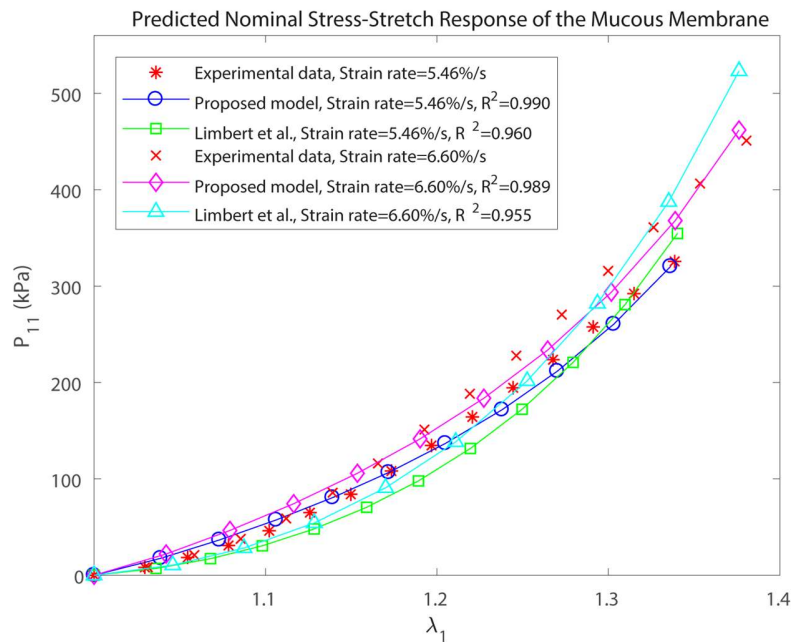

Figure 4. Comparison of the accuracy of prediction of the rate dependent response of the mucous tissue between the proposed model and Limbert's one.

As for the mucous tissue, the proposed CL is evaluated to predict the behavior of the bovine SLM. Equations (12a) and (13) are used to define the relationship between $\mathbf{P}$ and stretch in the muscle. The overall response to the external loading can be approximated by the sum of the resistance to the elongation of the matrix and of the fibers. To compute the contribution of each part, the quasi-static parameters c_{1-3} are calculated from the results of the two quasi-static (elastic) tensile tests with $\theta = 0°$ and $\theta = 20°$. Because $\mathbf{P}$ in the case of $\theta = 20°$ is not only a function of the controllable parameters of the machine, some complementary tools like a FEA has to be employed to determine the uncontrollable parameters of $\mathbf{F}$. So, the use of the FEA besides the results of the uniaxial tension tests leads to a complete determination of portions of the matrix and fibers in the resultant stress.

A first guess of the values of c_{1-3} are approximated from the results of tensile test along the direction of fibers, in which stress-stretch relationship can be simplified to a function of horizontal stretch F_{11} from equation (12a) and (13). The process is similar to elastic MPs estimation of the mucous membrane. Then, the tensile test with $\theta = 20°$ is simulated in ABAQUS explicit by implementing a user-defined material model in subroutine VUMAT. After the analysis, changes of the non-zero components of $\mathbf{F}$ during the loading time are ready to be used in $\mathbf{P}$. Thus, an updated values of c_{1-3} can be calculated by minimizing the differences between the measured and predicted stress values at $\theta = 0°$ and $\theta = 20°$ via a MATLAB script according to the Genetic algorithm. The proposed procedure of MPs estimation has to be iterated with the updated parameters to converge to constant values. Figure 5 shows the required steps to calculate the parameters of a transversely isotropic material via UTTs. The proposed method also can be used for materials with two families of fibers. For this case, the MPs converge to final values with more iterations on UTTs in various angles with respect to fibers directions.
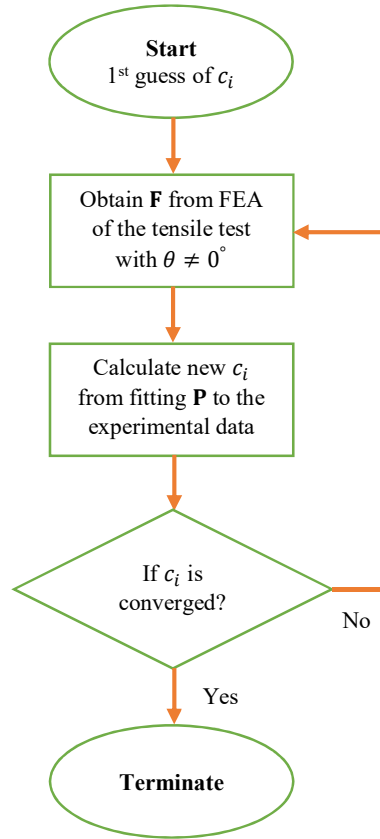
9

Figure 5. Flowchart of material parameters estimation procedure of a transversely isotropic material from uniaxial tensile tests.

Figure 6 shows the elastic response of the proposed model fitted to the experimental data points. The values of c_{1-3} have been determined by fitting the equation (12a) to the measured stress at $\theta = 0°$ and $\theta = 20°$. Figure 6 shows that the proposed CLs with the estimated MPs accurately predicts the elastic response of the SLM at $\theta = 35°$. In Table 2 the estimated MPs for this case are provided, in which they have converged to constant values after 5 iterations of the proposed procedure.

Table 2. Material parameters of the bovine superior longitudinal muscle tissue estimated for the proposed model and for Limbert's model.

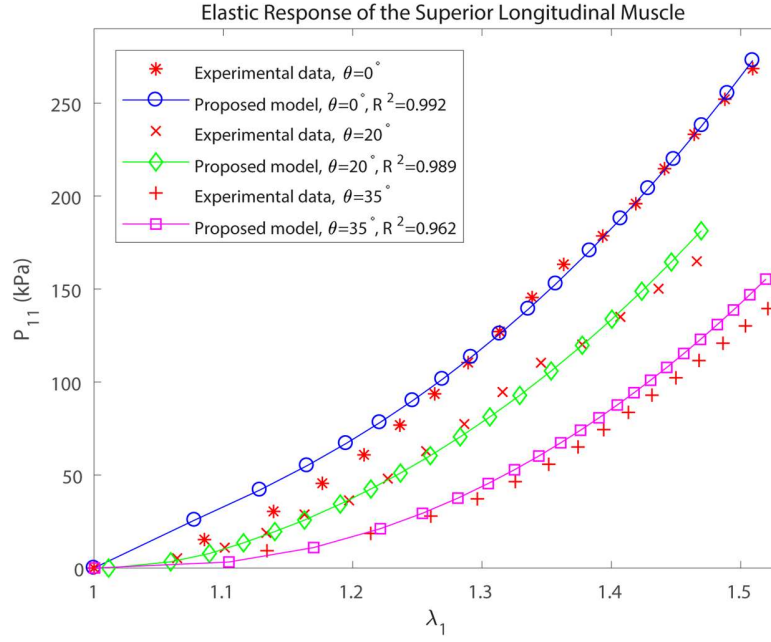|	c_1 (kPa)	c_2 (kPa)	c_3 (-)	c_4 (kPa)	c_5 (-)	a_1 (kPa)	a_2 (kPa)
Proposed model	38.081	47.863	1.773	1400	1.231	-	-
Limbert et al.	38.081	47.863	1.773	-	-	7079	0

Figure 6. Elastic response of the superior longitudinal muscle tissue to the uniaxial tension tests in different angles with the fibers direction. Similarly, the best approximation of the proposed model is depicted.

After determining the elastic MPs, to estimate the viscous behavior of the tissues, MPs $c_{4,5}$ and $a_{1,2}$ are computed by fitting the equations (12b), (13) and (17) to the stress-stretch data points of the tension test along the fibers ($\theta = 0°$) at a strain rate of 1.46%/s. The values of these parameters are reported in table 2. It is remarkable that the best fitted Limbert's model to the experimental data points does not share any contribution for the fibers in the viscous response of the SLM ($a_2 = 0$), unlike our model in equation (10b), in which the viscous part of stress has been restricted to the fibers effect.
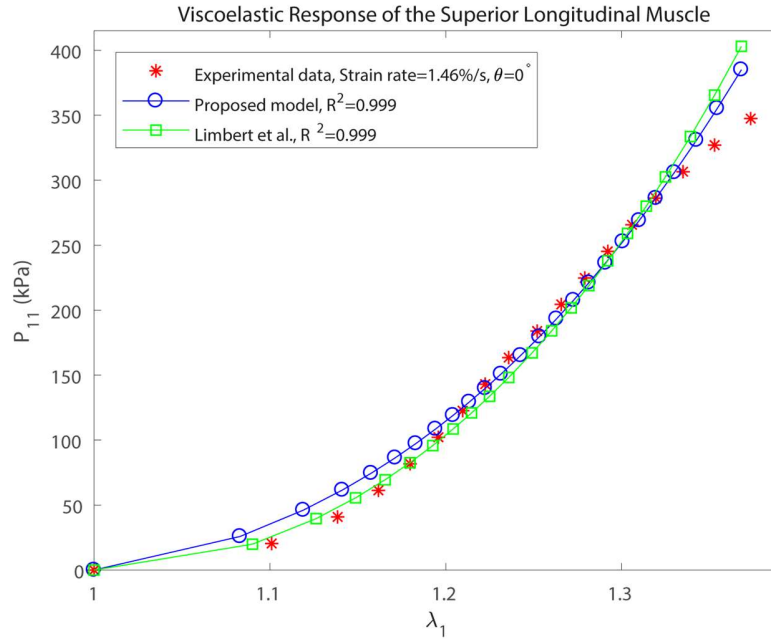
Figure 7. Fitting the proposed model and Limbert's model to the rate dependent
response of the superior longitudinal muscle tissue.

Finally, using these estimated MPs, the accuracy of the proposed model (equation 10) is compared with respect to Limbert's relationship at a strain rate of 1.65%/s and with $\theta = 20°$ with respect to the fibers. In this case, nominal stress versus stretch is plotted in figure 8. Both models have been implemented in the ABAQUS explicit software and nominal stresses at a point far away from the machine clips are plotted in figure 8.

It seems that the proposed model predicts significantly more accurately the viscoelastic and the fiber orientation dependent nature of the muscle tissues. This accuracy probably originates from the existence in our model of a more general nonlinear relationship between stress and the stretch and stretch rate. Also, the significant differences of the response predictions in figure 8 emphasize that the viscous response considerably depends more on the fibers than the matrix.
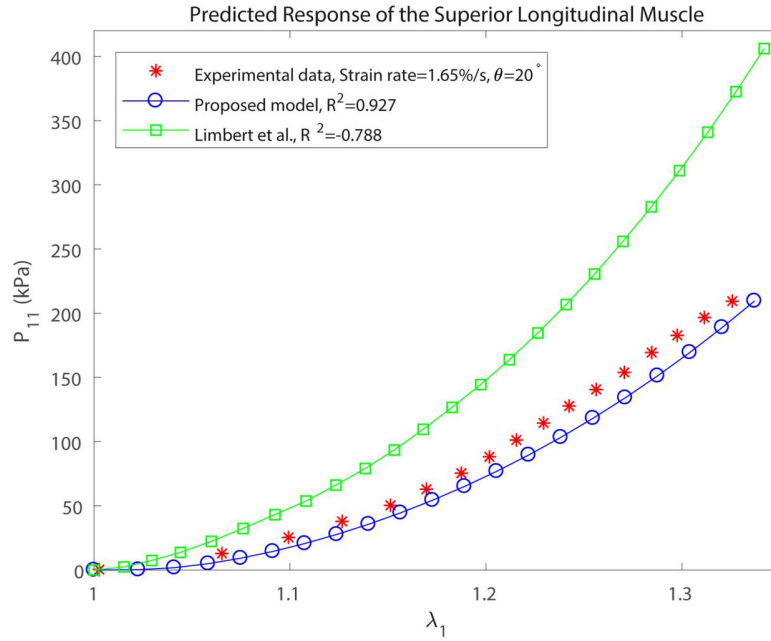
Figure 8. Comparison of the rate and orientation dependent responses of the
superior longitudinal muscle tissue between the proposed model and the one developed by Limbert et al.

Also, to show that the MPs are uniquely determined and there is not another set of the MPs that can provide an accurate prediction for the SLM, a demonstration has been given in Appendix A.

5. Discussions

During the last two decades, many researchers have studied tongue functions, but very few data were provided as concerns its material properties, in particular, the viscoelastic and anisotropic nature of its tissues. This paper has proposed to address this question by studying the mechanical response of bovine tongue tissues. Appropriate samples from the mucous part of the tongue were dissected and elongated uniaxially at different strain rates. Among the various muscle groups of the tongue, the SLM was chosen because of its ability to provide acceptable macroscopic samples. Such samples were tested at multiple strain rates and in various angles with respect to fibers' direction to determine the stress-stretch responses.

With the aid of inverse FE method, an iteration-based procedure of MPs estimation was proposed for materials with one or two families of fibers. Using the proposed procedure the mechanical properties of these families of materials can be determined via UTTs without any need for biaxial tests. According to this procedure, the material properties of the SLM of bovine tongue tissue did converge to the reported values with only 5 iterations.

Assuming the energy function as a general nonlinear relationship with respect to the stretch and the rate of stretch, two visco-hyperelastic CLs were proposed for the isotropic and transversely isotropic soft tissues, using the invariants of $\mathbf{C}$ and $\dot{\mathbf{C}}$. In addition, the proposed models incorporate the objectivity and convexity constraints for both strain energy function and potential viscous function.

The proposed models were implemented in ABAQUS explicit via a VUMAT subroutine. A good agreement between FEA results and experimental data points validates the estimated MPs of bovine tongue tissue. Compared to a reference visco-hyperelastic CLs presented by Limbert, for the isotropic mucous tissue in which the proposed model uses an extra material parameter, a slightly more accurate prediction

13

was obtained. For the transversely isotropic case, in which both the proposed relationship and Limbert's model use the same number of MPs, our model shows a better agreement with a larger domain of conformity. The proposed models account for large deformation, orientation dependent and viscous behaviors accurately and show their advantage for modeling the behavior of soft tissues.

Acknowledgements

References

Ahsanizadeh, S., & Li, L. (2015). Visco-hyperelastic constitutive modeling of soft tissues based on short and long-term internal variables. *Biomedical engineering online*, *14*(1), 29.

Boehler, J. P. (1987). *Applications of tensor functions in solid mechanics* (Vol. 292). J. P. Boehler (Ed.). New York: Springer.

Chagnon, G., Rebouah, M., & Favier, D. (2015). Hyperelastic energy densities for soft biological tissues: a review. *Journal of Elasticity*, *120*(2), 129-160.

Dang, J., & Honda, K. (2002). Estimation of vocal tract shapes from speech sounds with a physiological articulatory model. *Journal of Phonetics*, *30*(3), 511-532.

Davis, F. M., & De Vita, R. (2012). A nonlinear constitutive model for stress relaxation in ligaments and tendons. *Annals of biomedical engineering*, *40*(12), 2541-2550.

Davis, F. M., & De Vita, R. (2014). A three-dimensional constitutive model for the stress relaxation of articular ligaments. *Biomechanics and modeling in mechanobiology*, *13*(3), 653-663.

Fujita, S., Dang, J., Suzuki, N., & Honda, K. (2007). A computational tongue model and its clinical application. *Oral Science International*, *4*(2), 97-109.

Fung, Y. C. (2013). *Biomechanics: mechanical properties of living tissues*. Springer Science & Business Media.

Gérard, J. M., Ohayon, J., Luboz, V., Perrier, P., & Payan, Y. (2005). Non-linear elastic properties of the lingual and facial tissues assessed by indentation technique: application to the biomechanics of speech production. *Medical engineering & physics*, *27*(10), 884-892.

Gérard, J. M., Wilhelms-Tricarico, R., Perrier, P., & Payan, Y. (2006). A 3D dynamical biomechanical tongue model to study speech motor control. *arXiv preprint physics/0606148*.

Gilbert, R. J., Wedeen, V. J., Magnusson, L. H., Benner, T., Wang, R., Dai, G., ... & Roche, K. K. (2006). Three-dimensional myoarchitecture of the bovine tongue demonstrated by diffusion spectrum magnetic resonance imaging with tractography. *The Anatomical Record Part A: Discoveries in Molecular, Cellular, and Evolutionary Biology*, *288*(11), 1173-1182.

Gras, L. L., Mitton, D., Viot, P., & Laporte, S. (2012). Hyper-elastic properties of the human sternocleidomastoideus muscle in tension. *journal of the mechanical behavior of biomedical materials*, *15*, 131-140.

Hernández, B., Pena, E., Pascual, G., Rodriguez, M., Calvo, B., Doblaré, M., & Bellón, J. M. (2011). Mechanical and histological characterization of the abdominal muscle. A previous step to modelling hernia surgery. *Journal of the mechanical behavior of biomedical materials*, *4*(3), 392-404.

Holzapfel, G. A., & Ogden, R. W. (2010, June). Constitutive modelling of arteries. In *Proceedings of the Royal Society of London A: Mathematical, Physical and Engineering Sciences* (Vol. 466, No. 2118, pp. 1551-1597). The Royal Society.

Holzapfel, G. A. (2000). *Nonlinear solid mechanics* (Vol. 24). Chichester: Wiley.

Humphrey, J. D. (2003, January). Review Paper: Continuum biomechanics of soft biological tissues. In *Proceedings of the Royal Society of London A: Mathematical, Physical and Engineering Sciences* (Vol. 459, No. 2029, pp. 3-46). The Royal Society.

Kajee, Y., Pelteret, J. P., & Reddy, B. D. (2013). The biomechanics of the human tongue. *International journal for numerical methods in biomedical engineering*, *29*(4), 492-514.

Kulkarni, S. G., Gao, X. L., Horner, S. E., Mortlock, R. F., & Zheng, J. Q. (2016). A transversely isotropic visco-hyperelastic constitutive model for soft tissues. *Mathematics and Mechanics of Solids*, *21*(6), 747-770.

Li, S., Beyerlein, I. J., Necker, C. T., Alexander, D. J., & Bourke, M. (2004). Heterogeneity of deformation texture in equal channel angular extrusion of copper. *Acta materialia*, *52*(16), 4859-4875.

Limbert, G., & Middleton, J. (2004). A transversely isotropic viscohyperelastic material: application to the modeling of biological soft connective tissues. *International Journal of Solids and Structures*, *41*(15), 4237-4260.

Lu, Y. T., Zhu, H. X., Richmond, S., & Middleton, J. (2010). A visco-hyperelastic model for skeletal muscle tissue under high strain rates. *Journal of biomechanics*, *43*(13), 2629-2632.

Martins, J. A. C., Pires, E. B., Salvado, R., & Dinis, P. B. (1998). A numerical model of passive and active behavior of skeletal muscles. *Computer methods in applied mechanics and engineering*, *151*(3-4), 419-433.

Martins, J. A. C., Pato, M. P. M., & Pires, E. B. (2006). A finite element model of skeletal muscles. *Virtual and Physical Prototyping*, *1*(3), 159-170.

McLoon, L. K., & Andrade, F. (Eds.). (2012). *Craniofacial muscles: A new framework for understanding the effector side of craniofacial muscle control*. Springer Science & Business Media.

Nazari, M. A. (2011). *Biomechanical face modeling: control of orofacial gestures for speech production* (Doctoral dissertation, Université de Grenoble).

Ogden, R. W. (2009). Anisotropy and nonlinear elasticity in arterial wall mechanics. In *Biomechanical modelling at the molecular, cellular and tissue levels* (pp. 179-258). Springer Vienna.

Peña, J. A., Martínez, M. A., & Peña, E. (2011). A formulation to model the nonlinear viscoelastic properties of the vascular tissue. *Acta Mechanica*, *217*(1-2), 63-74.

Pioletti, D. P., Rakotomanana, L. R., Benvenuti, J. F., & Leyvraz, P. F. (1998). Viscoelastic constitutive law in large deformations: application to human knee ligaments and tendons. *Journal of biomechanics*, *31*(8), 753-757.

Pioletti, D. P., & Rakotomanana, L. R. (2000). Non-linear viscoelastic laws for soft biological tissues. *European Journal of Mechanics A-Solids*, *19*(LBO-ARTICLE-2000-002), 749-759.

Pioletti, D. P. (2006). Viscoelastic constitutive law based on the time scale of the mechanical phenomena. In *Mechanics of biological tissue* (pp. 399-404). Springer Berlin Heidelberg.

Rastadmehr, O., Bressmann, T., Smyth, R., & Irish, J. C. (2008). Increased midsagittal tongue velocity as indication of articulatory compensation in patients with lateral partial glossectomies. *Head & neck*, *30*(6), 718-726.

Spencer, A. J. M. (Ed.). (1984). *Continuum theory of the mechanics of fibre-reinforced composites* (Vol. 282). New York: Springer.

Takaza, M., Moerman, K. M., Gindre, J., Lyons, G., & Simms, C. K. (2013). The anisotropic mechanical behaviour of passive skeletal muscle tissue subjected to large tensile strain. *journal of the mechanical behavior of biomedical materials*, *17*, 209-220.

Vogel, A., Rakotomanana, L., & Pioletti, D. P. (2017). Visco-hyperelastic strain energy function. In Biomechanics of Living Organs: Hyperelastic Constitutive Laws for Finite Element Modeling. Elsevier.

Vogt, F. (2005). Finite element modeling of the tongue. In *AVSP* (pp. 143-144).

Wilhelms-Tricarico, R. (1995). Physiological modeling of speech production: Methods for modeling soft-tissue articulators. *The Journal of the Acoustical Society of America*, *97*(5), 3085-3098.

Zhurov, A. I., Limbert, G., Aeschlimann, D. P., & Middleton, J. (2007). A constitutive model for the periodontal ligament as a compressible transversely isotropic visco-hyperelastic tissue. *Computer methods in biomechanics and biomedical engineering*, *10*(3), 223-235.

Appendix A

## Uniqueness of the estimated Material parameters

The proposed CL to describe the passive behavior of the SLM in equation (10) has five material parameters c_{1-5}. Each of them represents a specific mechanical behavior of the SLM, c_{1-3} and $c_{4,5}$ in equation (10) are considered constituting the elastic and rate dependent responses, respectively. Furthermore, it has to be emphasized that their values are not determined at the same time and after the estimation of the coefficients c_{1-3}, $c_{4,5}$ can be determined. In the following, it has been demonstrated that the elastic material parameters have been determined uniquely. Then, a similar proof has been provided for the coefficients of equation (10b).

To describe the behavior of a transversely isotropic material, it is necessary to consider both of the matrix and fibers effects. Thus, at least two independent material parameters have to be used in a constitutive law. But the sufficiency of only two material parameters to accurately predicting the observed behavior depends on the shape of the measured stress-stretch curves in the experiments. According to this point, a 3-parameters model has been chosen to describe the elastic stress-stretch relationship in the SLM, equation (10a).

Basically, the possibility of leading to non-unique values of the material parameters in a specific model originates from using some additional material parameters which can be ignored without a significant decrease in the goodness of fitting. In another word, an extra material parameter provides some extra degrees of freedom to the curve which is not necessary for following the experimental data points. In the proposed model in equation (10a), c_1 is the only parameter which has been employed to represent the effects of the matrix in the material resistance and can't be ignored. Also, c_2 and c_3 represent the effect of the fibers and perhaps one of them being unnecessary. To examine the question, once c_2 has been disregarded ($c_2 = 1$) in the model and then c_3 has been treated similarly. Best curves fitted to the experimental data points, similar to the figure 6 of the article, under these conditions are depicted in figure A1.

From figure A1 it is obvious that a 2-parameters constitutive law roughly predicts the behavior of the SLM. Thus, it seems that at least a 3-parameters model can provide enough degrees of freedom to follow the experimental data points.

In addition, it is supposed to add an extra term like $c_6(I_1 - 3)^3$ to the proposed model in equation (10a) and the material parameters have to be tuned in this case. In another word, a 4-parameters constitutive law, representing the matrix property, is chosen for the elastic response of the SLM. For this case, two figures of the best fits like figure 6 in the article are depicted in figure A2.
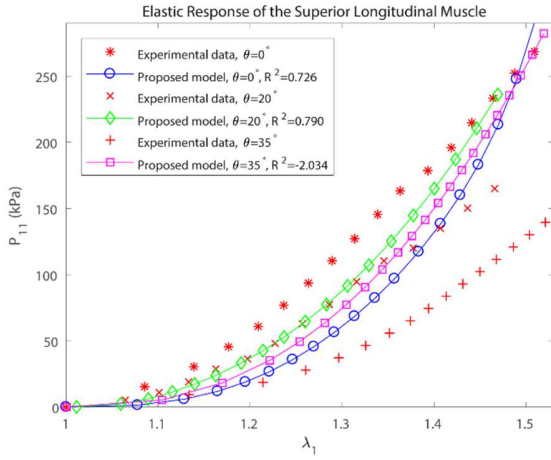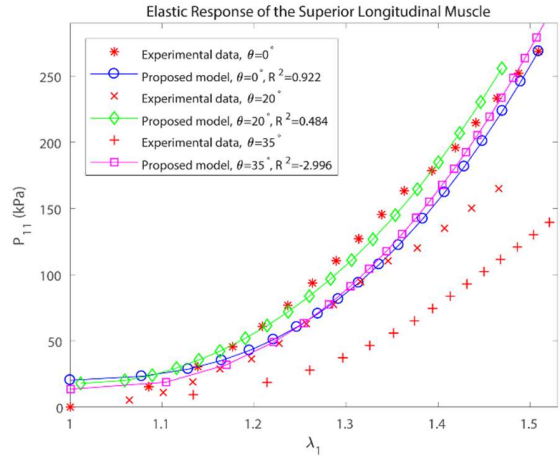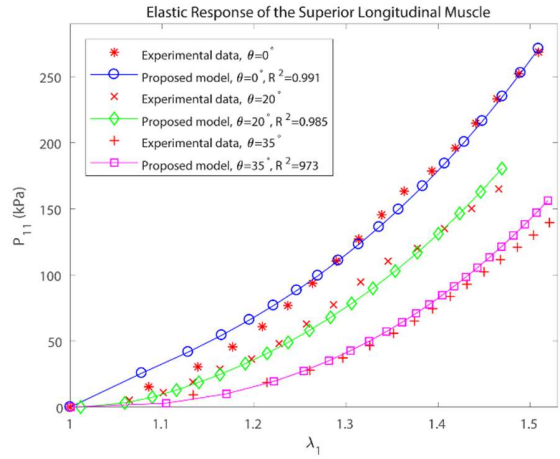
Figure A1. Best fitted curves to the elastic response of the SLM tissue when c_2 was ignored (a) and when c_3 was ignored (b).
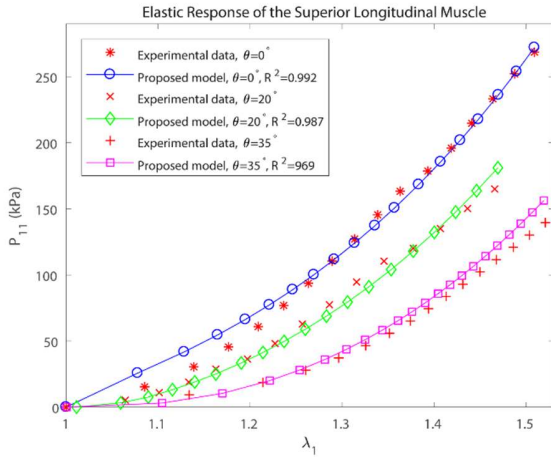
Figure A2. Best fitted curves to the elastic response of the SLM tissue when an extra term was added to equation (10a).

As it can be seen from figure A2, the figures can go on and on with different values of the material parameters because an extra degree of freedom was included in the model. So, it can be deduced that the three parameters are the minimum required number of material parameters in the proposed model to describe the elastic behavior of the SLM and they converged to the unique values which have been reported in the article.

Similar proofs to show that the rate dependent material parameters in equation (10b) have been uniquely determined can be provided here. It is supposed that there is no need for two independent material

parameters to predict the rate dependent behavior of the SLM. Thus, the goodness of fitting has to be examined when one of the c_4 or c_5 is disregarded. Like figure 7 in the article, the best fitted curves to the viscoelastic stress-stretch data points at θ=0^°are given in figure A3.

$$c_1 = 38.071, \quad c_2 = 47.863, \quad c_3 = 1.773$$
$$c_4 = 1, \quad c_5 = 0$$
(a)

$$c_1 = 38.071, \quad c_2 = 47.863, \quad c_3 = 1.773$$
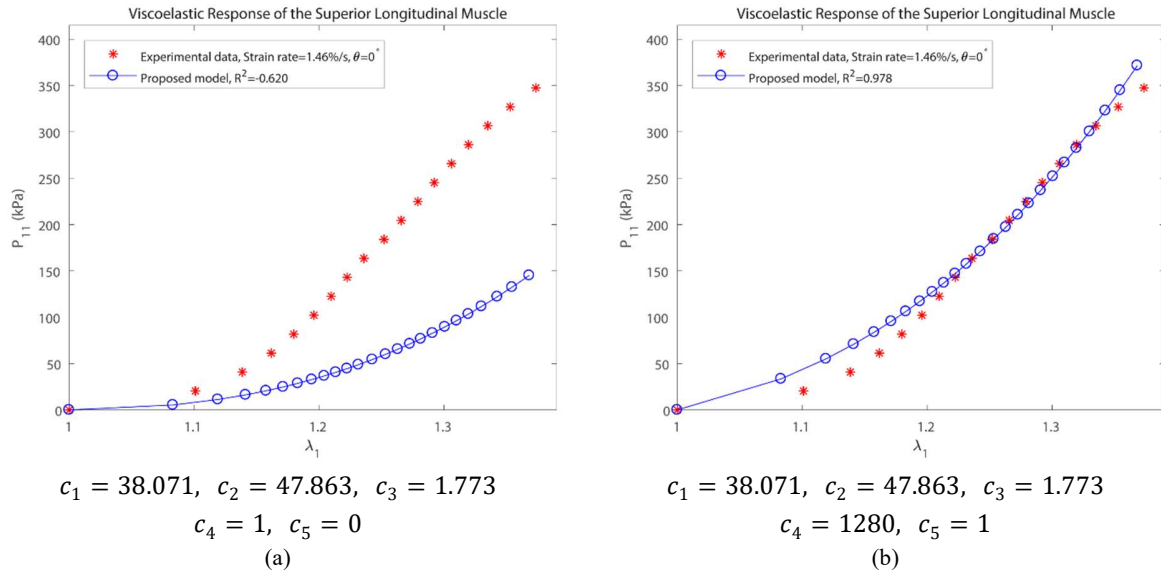$$c_4 = 1280, \quad c_5 = 1$$
(b)

Figure A3. Best fitted curves to the rate dependent response of the SLM tissue when c_4 was ignored (a) and when c_5 was ignored (b).

It seems that the fitted curve which is given in figure A3(b) accurately follows the experimental data points. But when it was examined to predict the response of the SLM in another direction, it did not result in an accurate prediction compared to the one has been reported in the article. So, it was decided to add the coefficient c_5 to the proposed model in equation (10b) to provide a better description to the soft tissues.